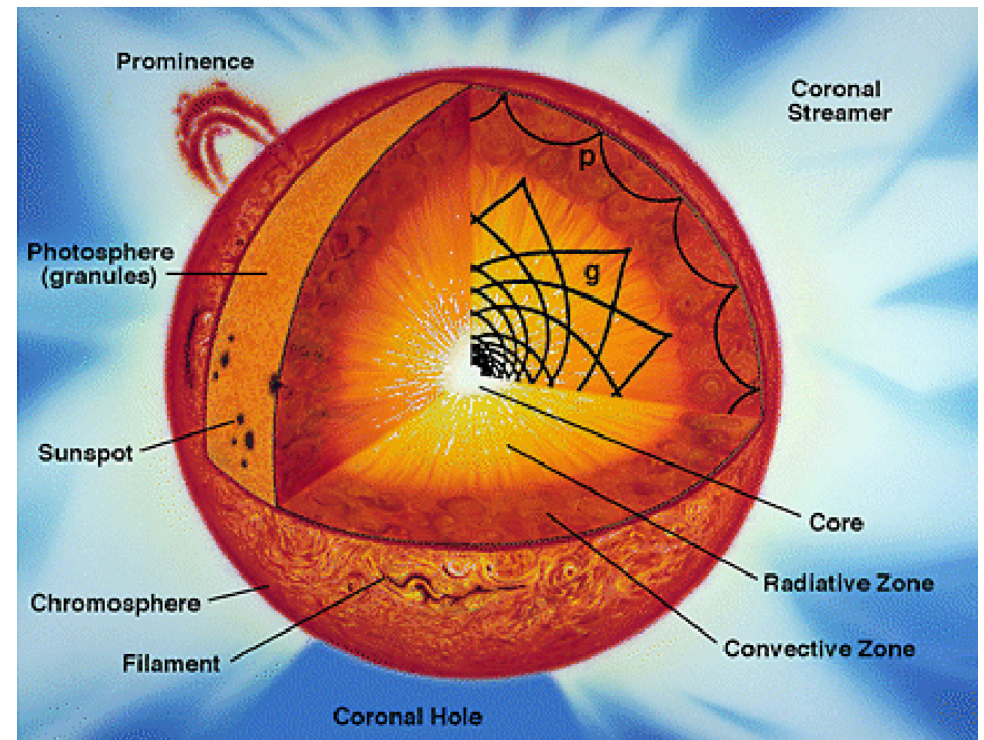


Mode selection in helioseismology

T. Corbard
OCA / Lagrange / UNS

Mode selection in helioseismology

- G (ravity) Modes - restoring force is buoyancy - internal gravity waves
- P (ressure) Modes - restoring force is pressure
- F (undamental) Modes - restoring force is buoyancy modified by density interface - surface gravity waves



Fundamental aspects of Solar oscillations used for the identification of the normal modes

- To a good approximation the Sun is spherically symmetric (oblateness $< 10^{-5}$).
- The (sidereal) rotation period (25 days) \gg 5 mn solar oscillations

=> Oscillations and departure from spherical symmetry (e.g. rotation) can be treated as small perturbations to the spherically symmetric model

=> the scalar quantities (pressure, temperature, etc.) associated with a single mode vary at the surface according to:

$$q = q_0 Y_l^m(\theta, \phi) e^{-i \omega t}$$

Fundamental aspects of Solar oscillations used for the identification of the normal modes

- Velocity vector on the solar surface

$$\mathbf{V}(\theta, \phi, t) = \sum_{n\ell m} \Re \{ V_r Y_\ell^m \mathbf{a}_r + V_h (\partial_\theta Y_\ell^m \mathbf{a}_\theta + 1/\sin\theta \partial_\phi Y_\ell^m \mathbf{a}_\phi) e^{-i\omega t} \}$$

- For low-degree modes with periods shorter than about an hour, the velocity field is predominantly in the radial direction

$$V(\theta, \phi; t) = \sqrt{4\pi} \Re \{ V_0 Y_l^m(\theta, \phi) \exp[-i(\omega_0 t - \delta_0)] \mathbf{a}_r \}$$

- Observations are only sensitive to the line-of-sight component of velocity $\rightarrow v_{\text{los}}$

Fundamental aspects of Solar oscillations used for the identification of the normal modes

- The amplitude associated with any single oscillation mode is very small
 - A few cm s^{-1} in velocity
 - A few part in 10^6 (ppm) for the relative intensity
(~ 4 mK in temperature, 10^{-4} arcseconds in radius)
- Many ($> 10^7$?) distinct oscillation modes are excited within the relatively narrow band 2-5 mHz
 - => confusion between modes is possible

Fundamental aspects of Solar oscillations used for the identification of the normal modes

- P-modes are damped modes that are excited stochastically by convection

=> for a single damped mode the velocity behave as :

$$\xi(t) = Ae^{(i\omega - \Gamma)t + i\delta}$$



$$\frac{1/4}{(\omega - \omega_0)^2 + \Gamma^2}$$

x

The Fourier transform of $Ae^{i\delta}$ depends on the excitation mechanism but is a slowly varying function of ω

=> Fitting Lorentzians to the Fourier transform of the time series

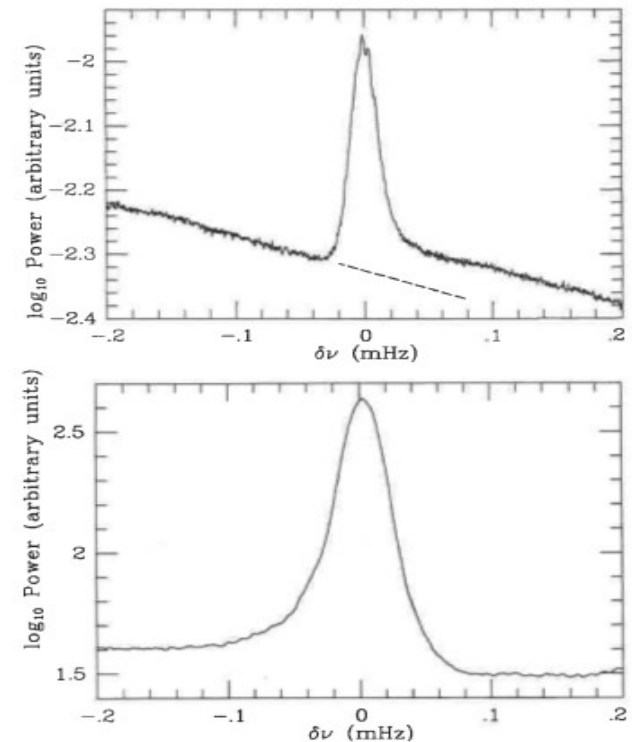
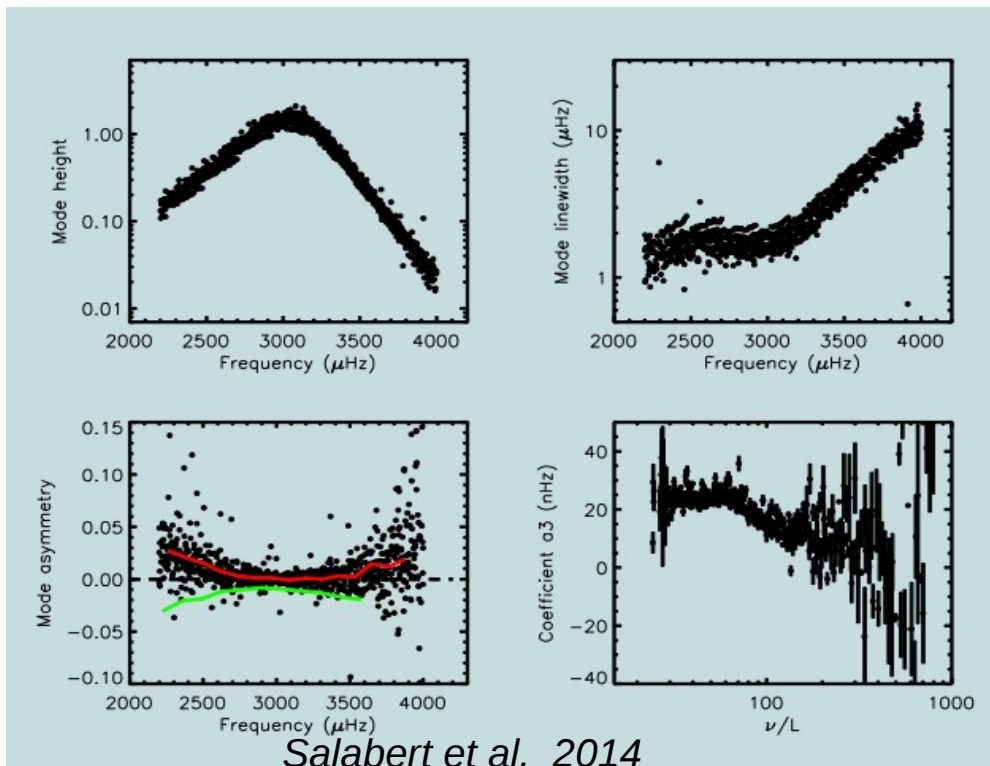
Fundamental aspects of Solar oscillations used for the identification of the normal modes

- However the observed profiles show assymetries of opposite sign in velocity and intensity measurements.

This results from the fact that one source of noise, the solar granulation, is correlated with oscillations

$$P(x) = A^2 \frac{(1 + Bx)^2 + B^2}{1 + x^2} + N_{\text{unc}}^2$$

$$x \equiv 2(\omega - \omega_{nlm})/\Gamma.$$



Data Reduction Methods – Preliminary Reduction

Raw data → standard maps of Doppler shift (or relative intensity)

- (1) Classical correction for gain and dark current variations in the instrument detector
- (2) Raw data to velocity conversion (depend on the instrument)

$$\delta v = \frac{I_{red} - I_{blue}}{I_{red} + I_{blue}}$$

- (3) Image registration and centering.

-->Compensate from telescope drive errors, pointing jitter, atmospheric seeing.

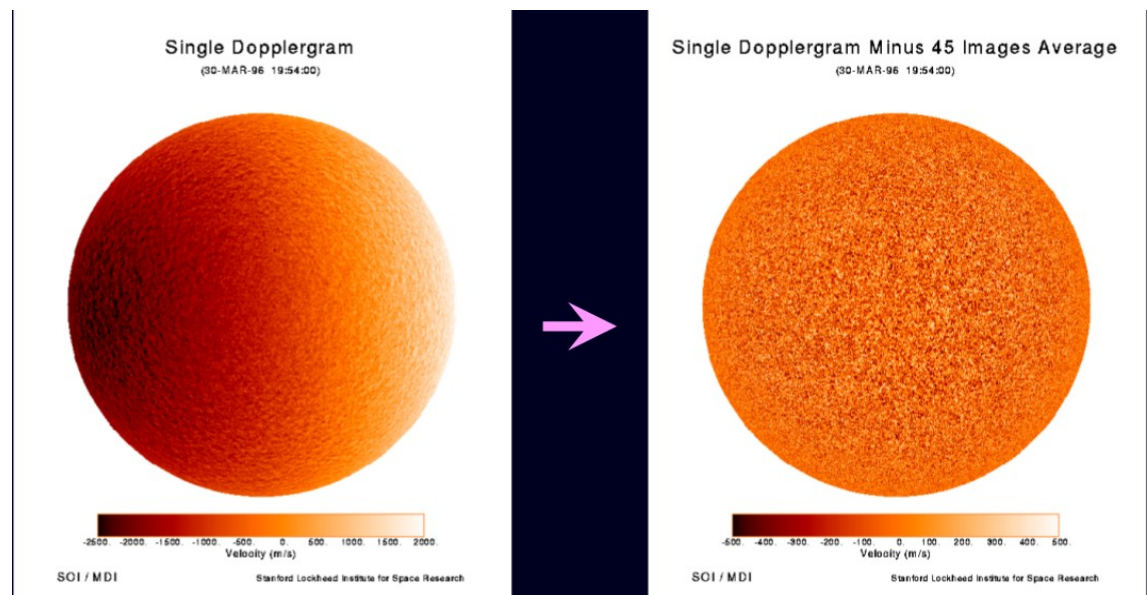
-->Poorly registered images will introduce blurring which lower sensitivity to high degree modes

-->Also needed for spherical harmonic transform

Method : limb fitting to determine the image center within 1/10 of a pixel and interpolation to shift the image

- (4) Remove known source of signal that are not relevant to the oscillations

- Sun's differential rotation
- Earth's rotation and orbital motion
- granulation

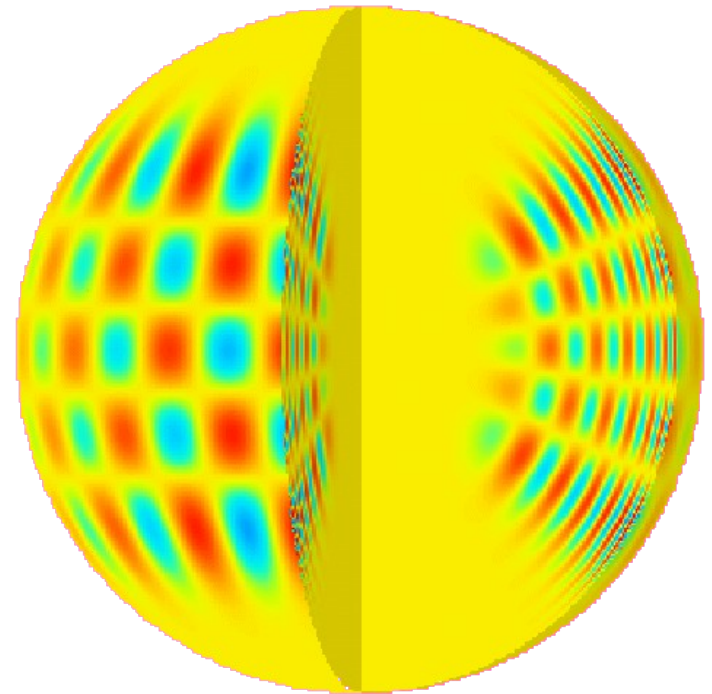
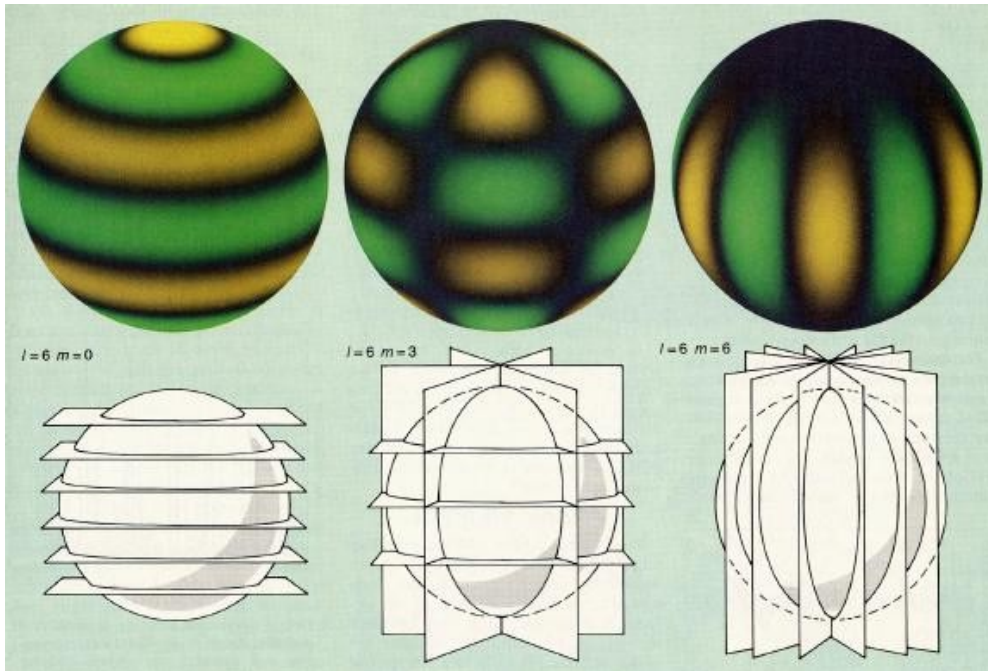


Data Reduction Methods - Spatial Filtering

$l=6 \ m=0$

$l=6 \ m=3$

$l=6 \ m=6$



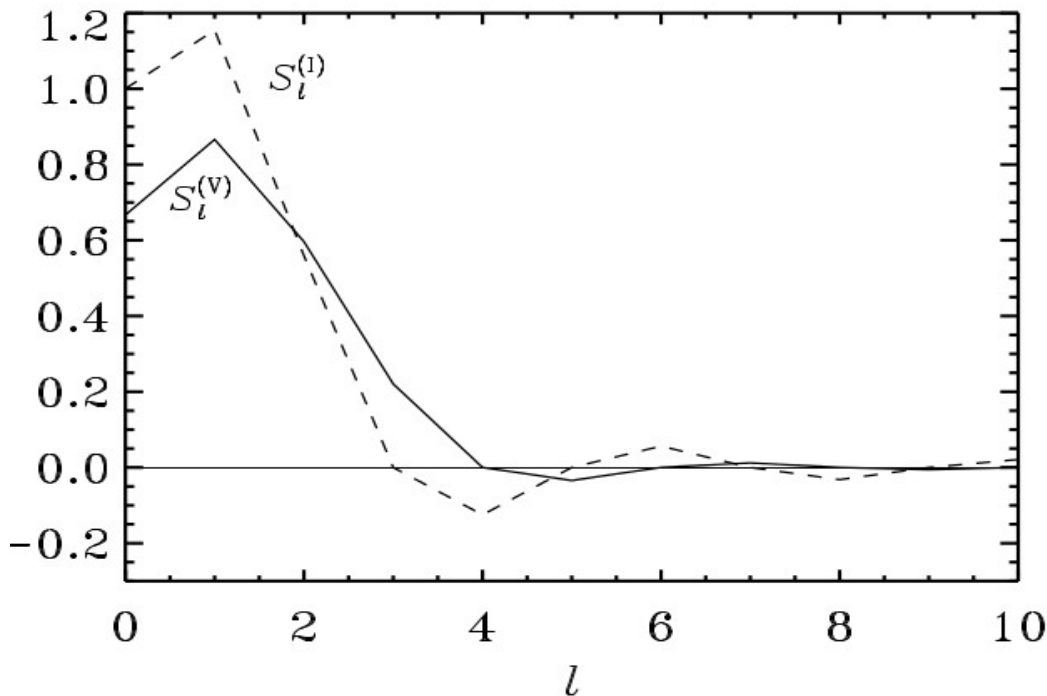
⇒ The goal is to isolate all the modes with the same surface pattern (l,m)

These modes with a given (l,m) will have different radial order n depending on their radial structure, inner turning point.

$$v_{\text{rad}}(r, \theta, \phi) = f_{nl}(r) Y_l^m(\theta, \phi)$$

Data Reduction Methods - Spatial Filtering

Case of full disk integration (non resolved)



Christensen-Dalsgaard, 2003

$$S'_{lm} = \Gamma_{lm} S_l,$$

$$\Gamma_{00} = 1$$

$$\Gamma_{11} = \frac{1}{\sqrt{2}}$$

$$\Gamma_{20} = \frac{1}{2}$$

$$\Gamma_{22} = \frac{\sqrt{6}}{4}$$

$$\Gamma_{31} = \frac{\sqrt{3}}{4}$$

$$\Gamma_{33} = \frac{\sqrt{5}}{4}$$

Γ_{lm} is zero when $l - m$ is odd.

$$\Gamma_{l-m} = \Gamma_{lm}.$$

Data Reduction Methods - Spatial Filtering

Spherical Harmonic Transform (SHT)

Any scalar function on sphere can be expanded in spherical harmonics

For simplicity, we assume we observe the radial velocity (rather than the line-of-sight velocity)

$$v(\theta, \phi, t) = \sum_{lm} A_{lm}(t) Y_l^m(\theta, \phi)$$

$$Y_l^m(\theta, \phi) = P_l^m(\cos \theta) e^{im\phi}$$

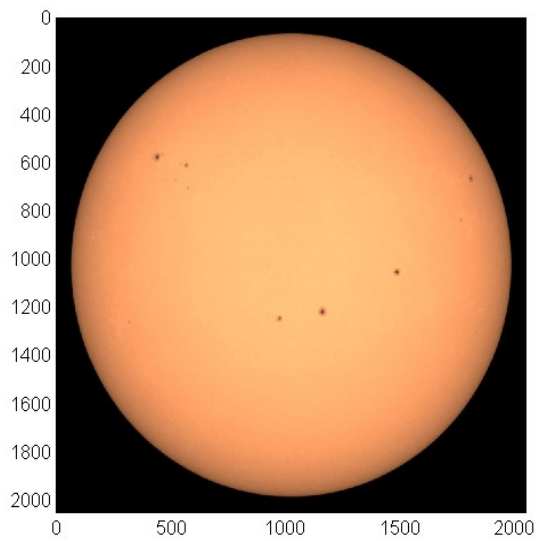
$$A_{lm}(t) = \int a_{lm}(\omega) e^{i\omega t} d\omega$$

$$v(\theta, \phi, t) = \sum_{lm} \int d\omega a_{lm}(\omega) Y_l^m(\theta, \phi) e^{i\omega t}$$

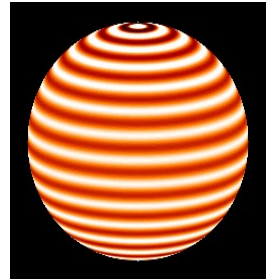
$$a_{lm}(\omega) = \frac{1}{2\pi} \int d\Omega dt v(\theta, \phi, t) Y_l^{m*}(\theta, \phi) e^{-i\omega t}$$

SHT: direct multiplication method

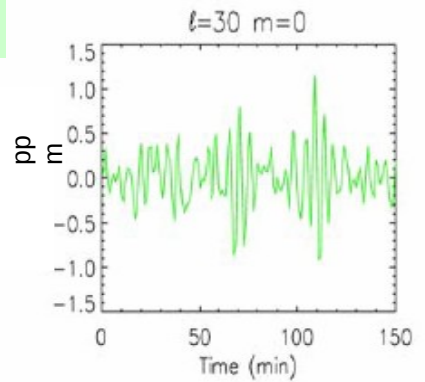
$$a_{lm}(\omega) = \frac{1}{2\pi} \int d\Omega dt v(\theta, \phi, t) Y_l^{m*}(\theta, \phi) e^{-i\omega t}$$



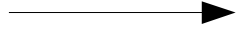
X



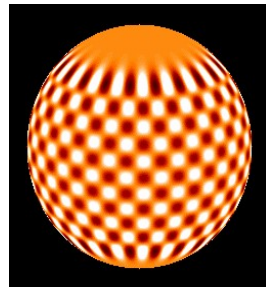
=



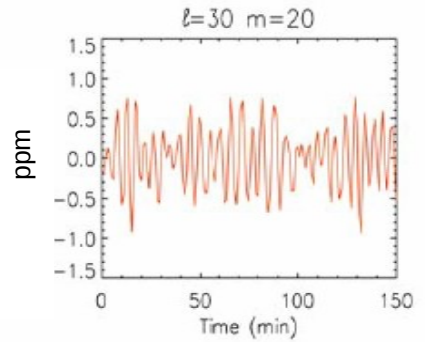
FFT



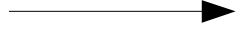
X



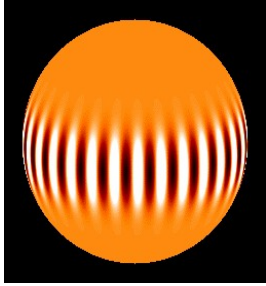
=



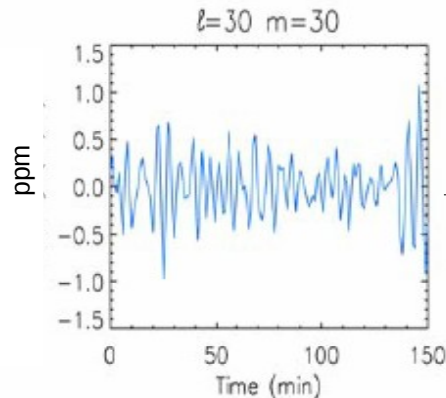
FFT



X



=



FFT



Each mask can be computed on an oversampled grid given each image geometry (P-angle, B0 angle, radius). Computationally expensive.

SHT: Fast method using FFTs

$$a_{lm}(\omega) = \frac{1}{2\pi} \int d\Omega dt v(\theta, \phi, t) Y_l^{m*}(\theta, \phi) e^{-i\omega t}$$

$$a_{lm}(\omega) = \frac{1}{2\pi} \iiint (v(\theta, \Phi, t) e^{-im\Phi}) d\Phi P_l^m(\cos\theta) \sin\theta d\theta e^{-i\omega t} dt$$

$$V_m(\theta, t) = \int v(\theta, \Phi, t) e^{-im\Phi} d\Phi$$

$$A_{lm}(t) = \int V_m(\theta, t) P_l^m(\cos\theta) \sin\theta d\theta$$

$$a_{lm}(\omega) = \int A_{lm}(t) e^{-i\omega t} dt$$

FFT in azimuth

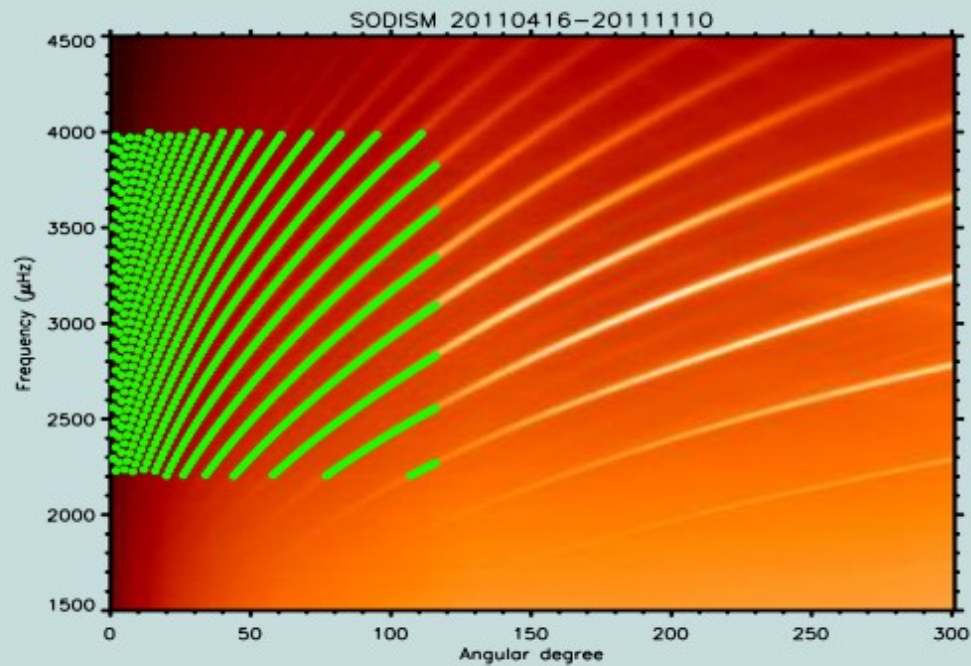


Legendre transform

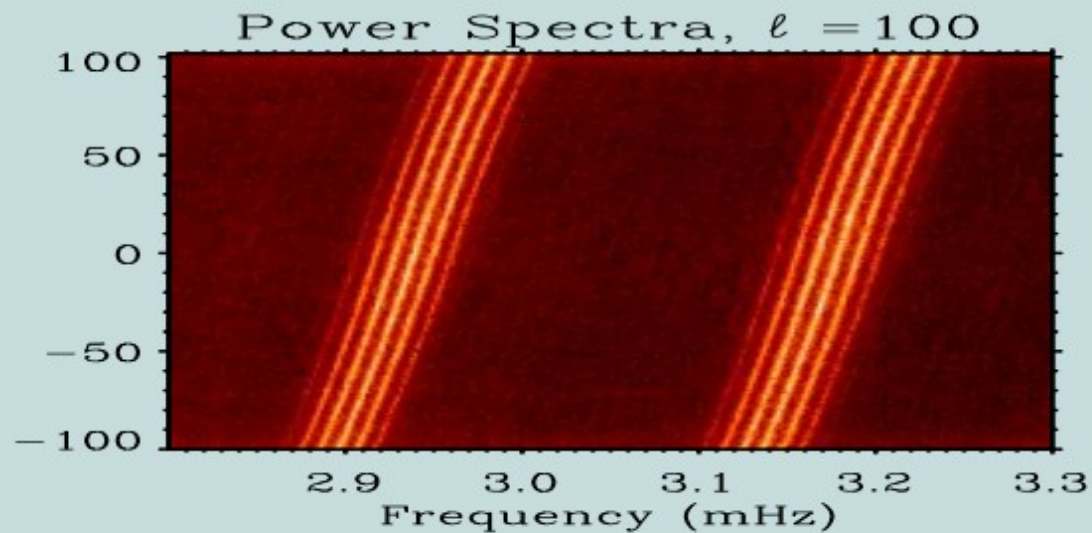


FFT in time

Faster but need an interpolation on a grid equally spaced in longitude and sine latitude => The quality of the image registration step is more important



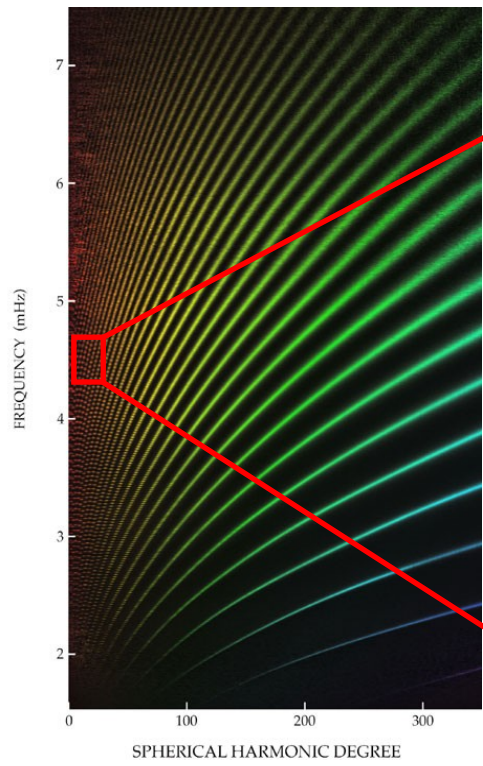
l-v Diagram



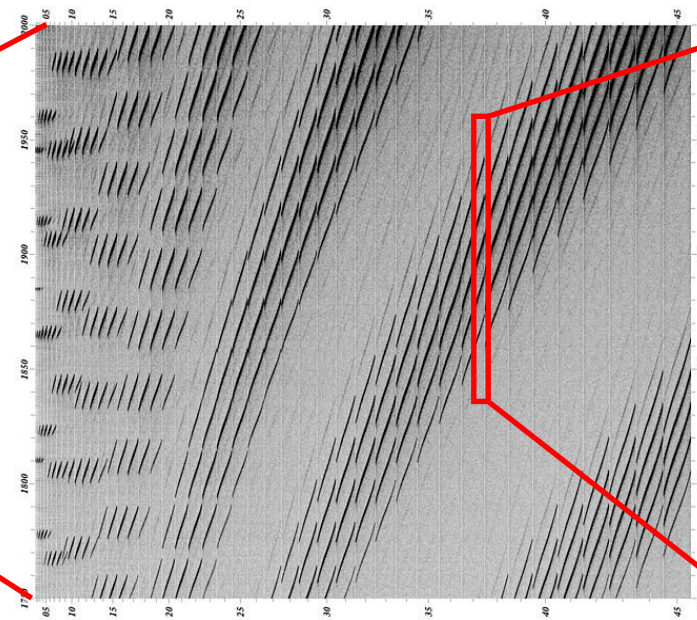
m-v Diagram

Fig 1: Top: l - v diagram from 209-day observations. The fitted modes are shown by the green dots.

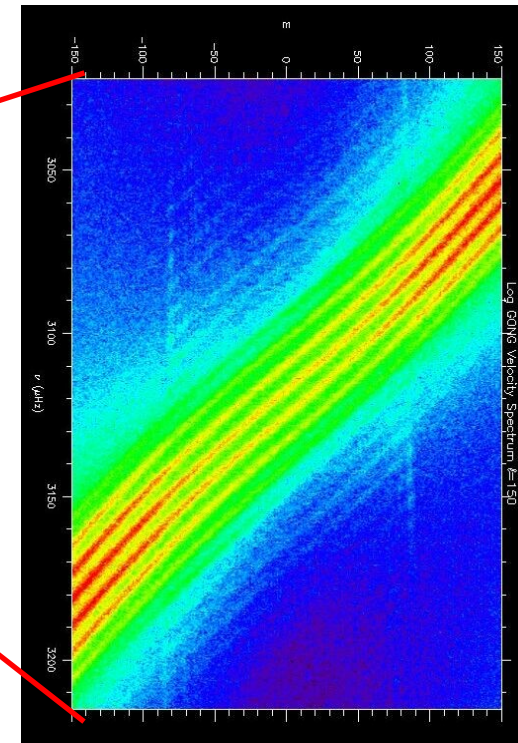
Bottom: m - v diagram for $l=100$ and radial order $n=6$ (left) and $n=7$ (right). The l -leaks from $l=100\pm 3$ are clearly seen.



l-*v* Diagram



l-*m*-*v* Diagram



m-*v* Diagram

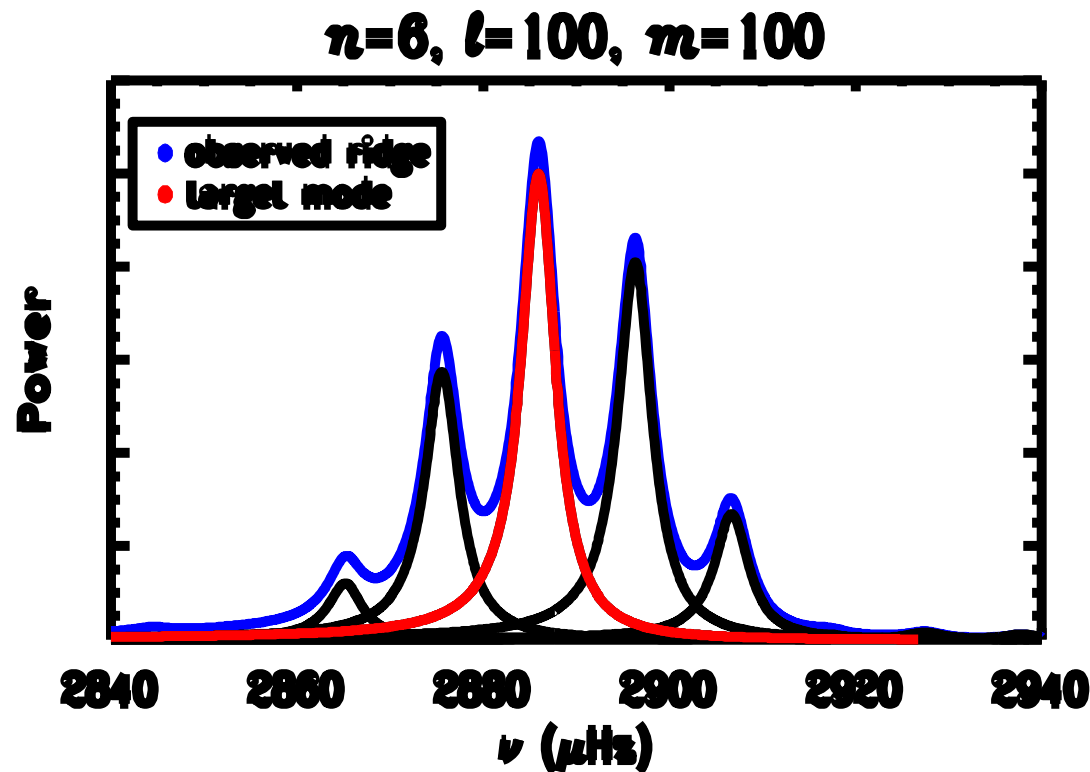
What is mode leakage?

$$A_{\ell,m}(t) = \int_{\theta} \int_{\phi} v_{\text{obs}}(\theta, \phi, t) M_{\ell,m}(\theta, \phi) d\phi d\theta$$

$$M_{l,m} \propto Y_{l,m}(\theta, \phi) A(\rho),$$

$$\rho \equiv \sqrt{\cos^2 \theta + \sin^2 \theta \sin^2 \phi} \quad V = \sqrt{1 - \rho^2}$$

- because we are unable to observe the whole solar surface (only less than half of the surface),
 - because of the appodisation
 - because of the projection factor
- ... the filters are not perfect and spurious modes leak into the filtered data.



Leakage matrix is the relative amplitude of the spurious modes present in a given (ℓ, m) power spectrum.

Leakage matrix

$$s(l, m, l', m') = \frac{1}{\pi} \int_{-1}^1 \int_{-\pi/2}^{\pi/2} P_l^m(x) P_{l'}^{m'}(x) \cos(m\phi) \cos(m'\phi) V(\rho) A(\rho) dx d\phi.$$

- leaks with odd $|\delta l + \delta m|$ (where $\delta m \equiv m - m'$ and $\delta l \equiv l - l'$) are not allowed.
- m-leaks ($\delta l = 0, \delta m = \pm 2$) is important to the estimation of low-degree splittings
- they are also asymmetrical : the $m = 1$ peak has an $m = 1 - 2$ leak on one side and no counterbalancing $m = 1 + 2$ leak on the other.
this can introduce a serious systematic error into the estimate of the splitting if not properly accounted for.
- the most deleterious effects arise when the leaks cannot be resolved from the target peaks (m-leaks at frequencies above about 2 mHz)
- for higher-degree modes l-leakage becomes a problem, as the ridges become both broader, and more closely spaced in frequency

How to get a good estimation of the leakage matrix?

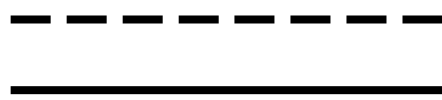
- With MDI and HMI we learned that:
 - Horizontal component is important (for velocity observations)
 - Distortion of the eigenfunctions by the solar rotation (Woodard 1989) is also important.
 - Good knowledge of the properties of the instrument (focus change, CCD tilt, image scale, radial distortion...)

Larson & Schou (2007)

Rabello-Soares et al.

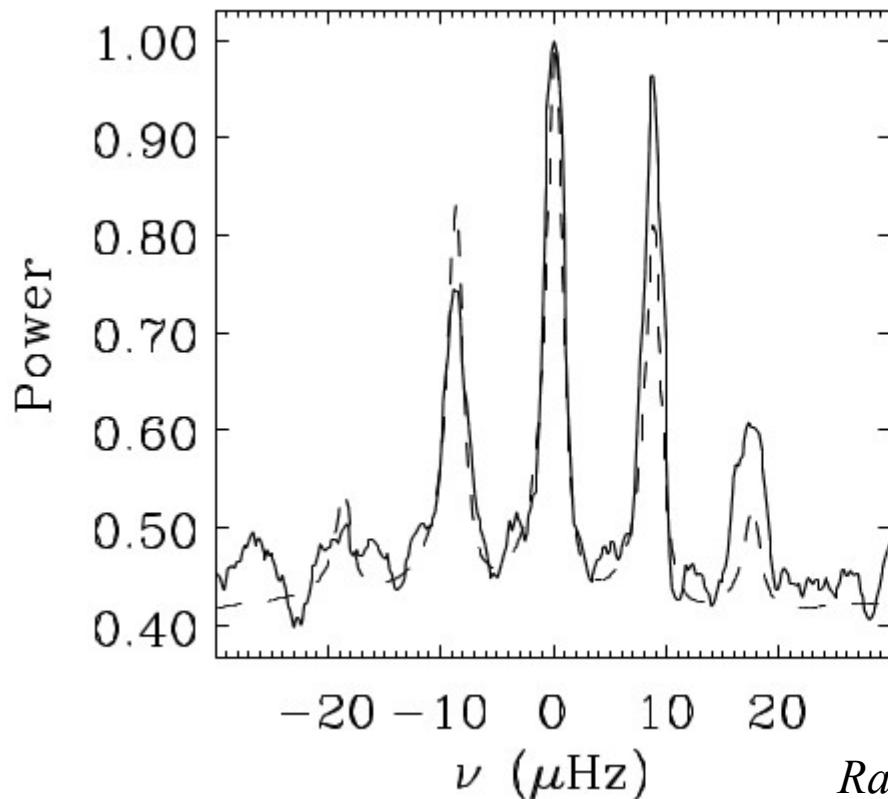
Effect of the horizontal component

$$\ell=77, m=77, n=2$$

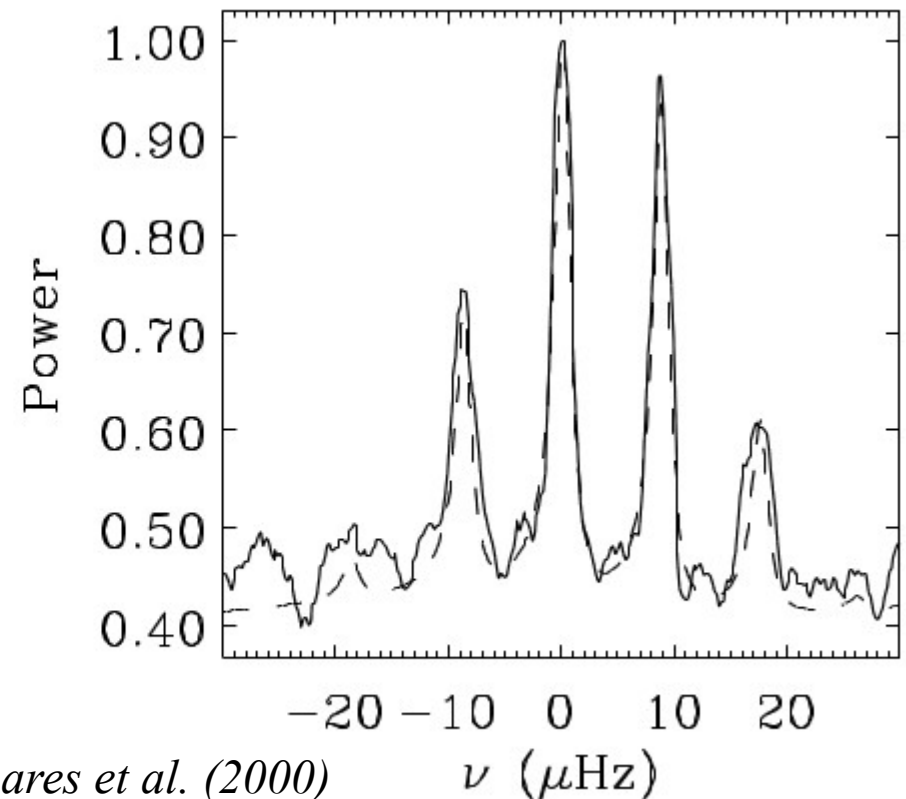


Model (using the leakage matrix)
Observed spectrum

NOT including horiz. component

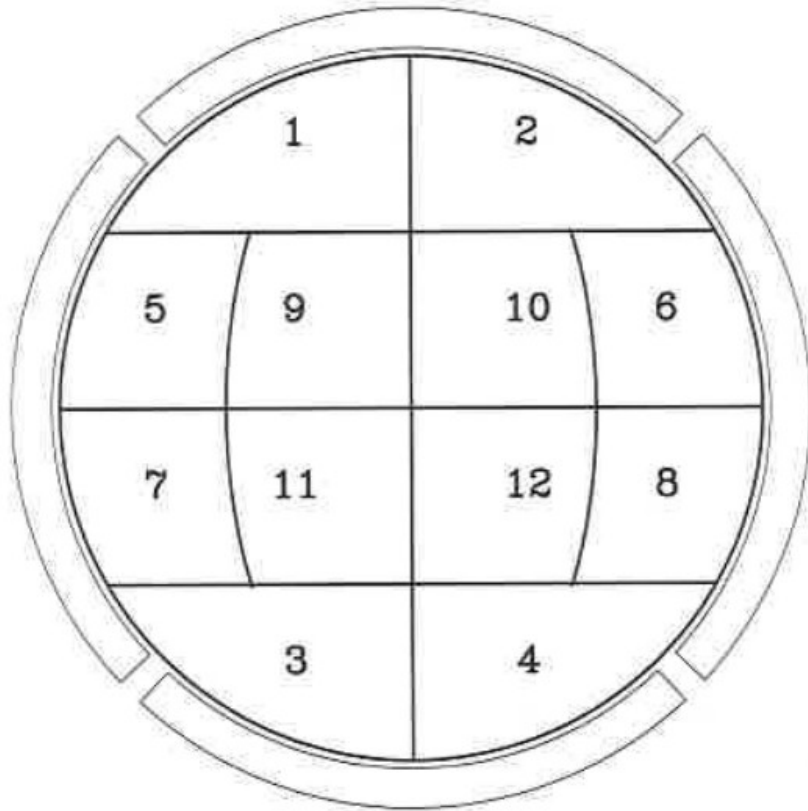


Including horiz. component



Rabello-Soares et al. (2000)

Another approach : Optimal Mask design



**What is the mode sensitivity
for this detector ?**

What are the optimal mask?

Fig. 1.4 The detector for the VIRGO-LOI experiment, with 12 central 'pixels' designed to be sensitive to modes with $l < 6$, plus an annulus of 4 detectors used for centering on the solar disc (guidance). (figure based on [Appourchaux *et al.* (1997)]).

Another approach : Optimal Mask design

Intensity / velocity signal seen in pixel i : $I_i = \int_{D_i} d \cos \theta d\phi I(\mu) \mu^q$ q=1 intensity
q=2 velocity

$$I(\mu) = I_0(\mu) \left[1 + \sum_{lm} I_l^m Z_l^m(\theta, \phi) \right]$$

Intensity / velocity signal from mode (l,m) seen in pixel i : $S_i(l, m) = \int_{D_i} d \cos \theta d\phi I(\mu) Z_l^m(\theta, \phi) \mu^q$

Sensitivities :

$$S(l, m) = \sqrt{\left[\sum_i S_i(l, m) \right] \left[\sum_i S_i^*(l, m) \right]}$$

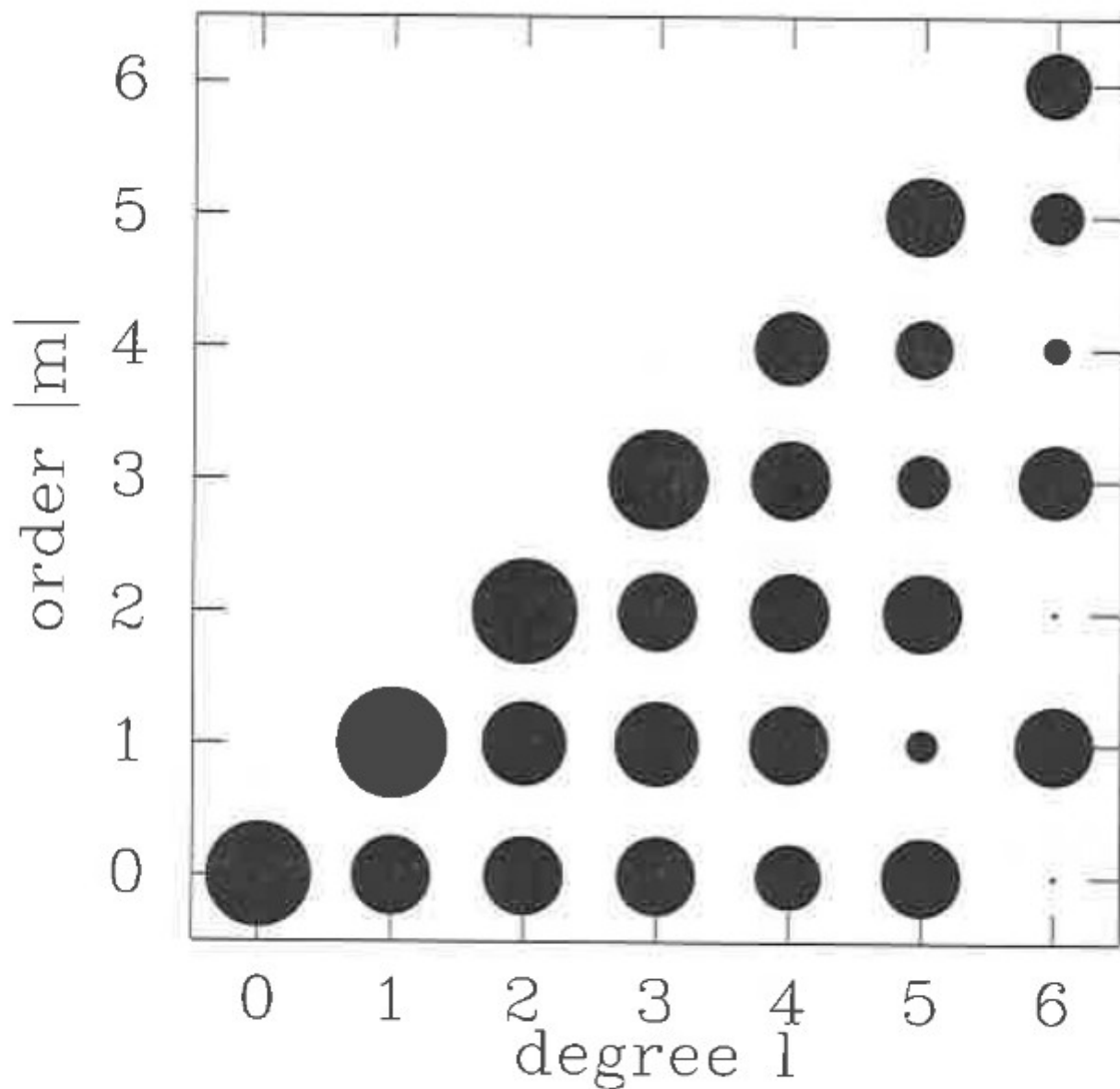


Fig. 1.5 The size of the symbols is proportional to the sensitivity of the VIRGO-LOI detector shown in Fig. 1.4. This is the sensitivity in intensity to a range of p-modes with low l, m . (figure based on [Appourchaux & Andersen (1990)]).

Optimal mask design as a linear discrete inverse problem

find linear weights a_i such that :

$$\sum_{l, m} \sum_i a_i(l_0, m_0) S_i(l, m) \approx I_{l_0}^{m_0} \delta_{l, l_0} \delta_{m, m_0}$$

e.g. SOLA method minimizing for the a_i :

$$\sum_{l, m} \left\{ \sum_i a_i(l_0, m_0) S_i(l, m) - \mathcal{T}(l - l_0, m - m_0) \right\}^2 + \mu_e \sum a_i a_j E_{ij}$$

THANKS !